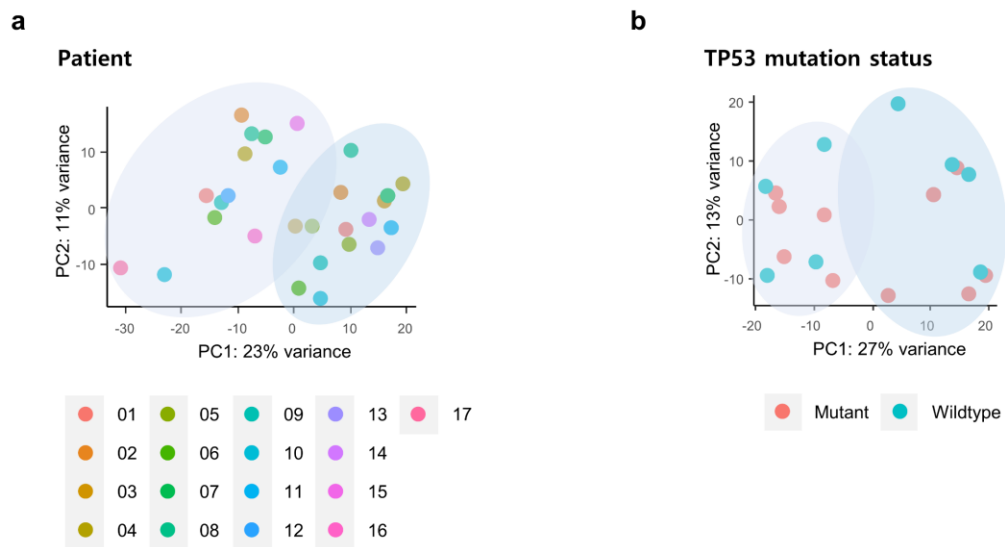**Supplementary Figure 1**

PCA plots of correlations within NanoString samples. a, PCA plot for 28 samples by individual patient. **b**, PCA plot for the 18 adenocarcinoma cases according to TP53 mutation status.
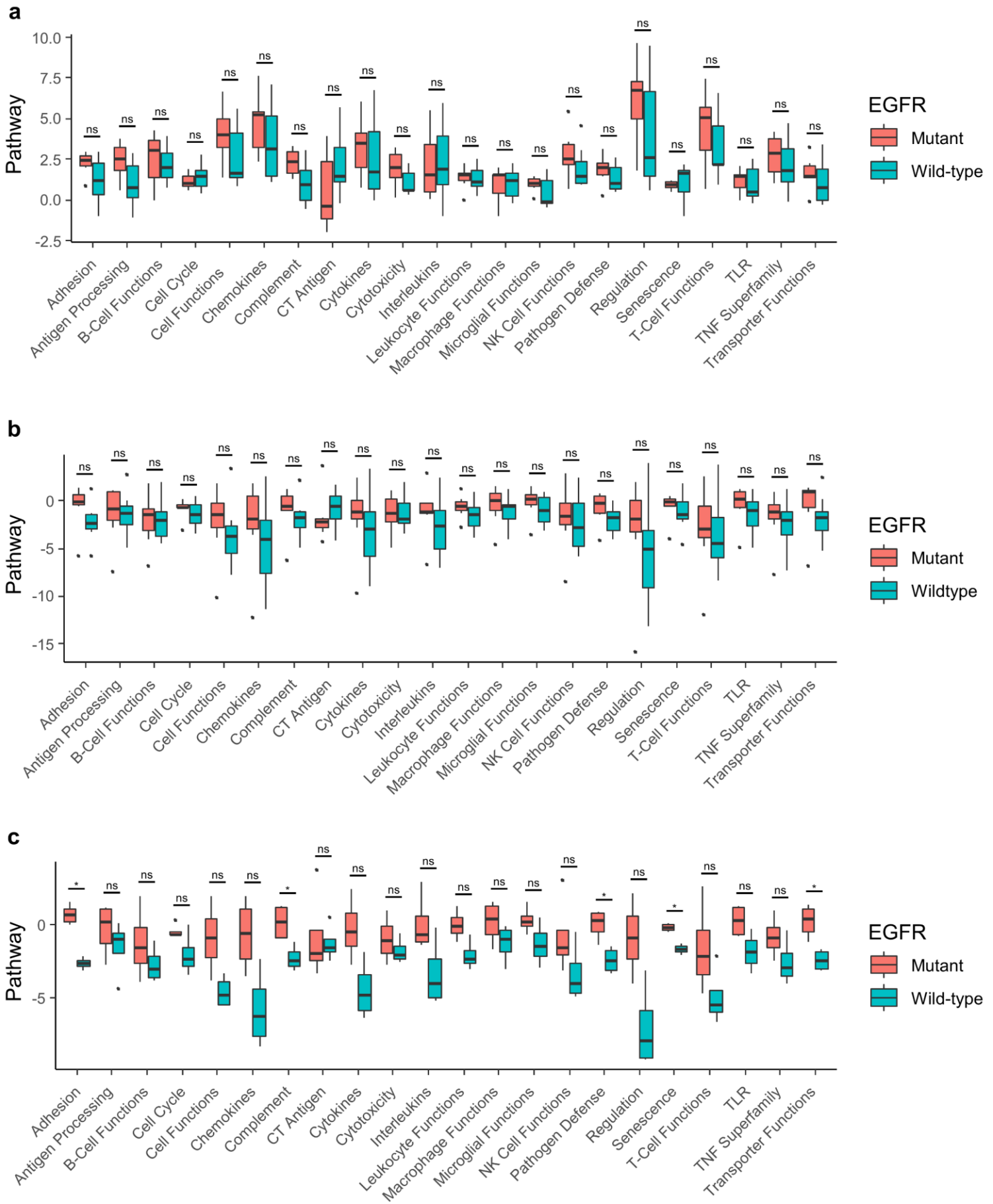
Supplementary Figure 2

Immunophenotypic differences in the lung and brain according to *EGFR* mutation status. a, Immune scores in *EGFR* wild-type versus *EGFR* mutant primary lung samples (Mann–Whitney U-test). **b,** Immune scores in *EGFR* wild-type versus *EGFR* mutant LCBM cases (Mann–Whitney U-test). **c,** Immune scores in *EGFR* wild-type versus *EGFR* mutant LCBM adenocarcinoma cases with no previous tyrosine kinase inhibitor treatment (Mann–Whitney U-test). CT antigen, cancer/testis antigen; TLR, Toll-like receptor; ns, not significant.
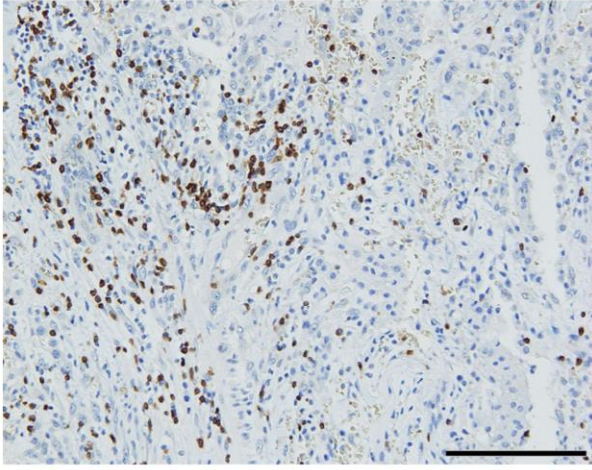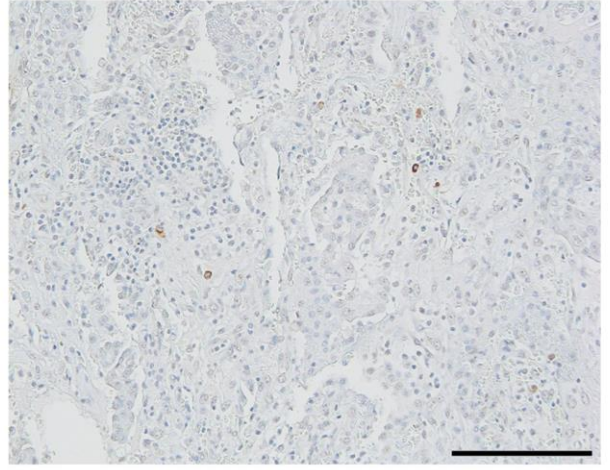
Supplementary Figure 2

Supplementary Figure 3

Comparative immunohistochemical images of CD3, NCR1, iNOS, and CD163 in representative primary lung and brain metastatic samples. Scale bar, 100 μm.
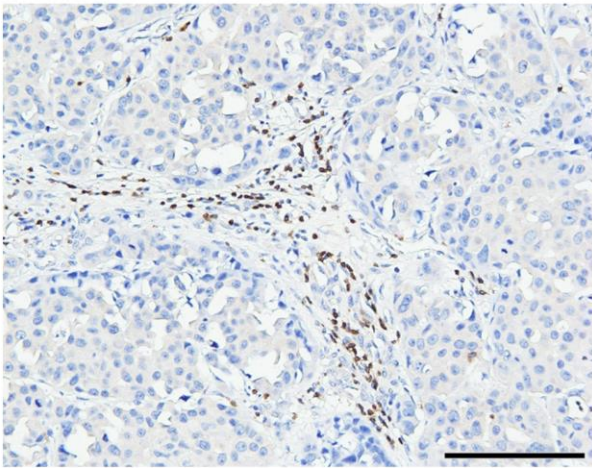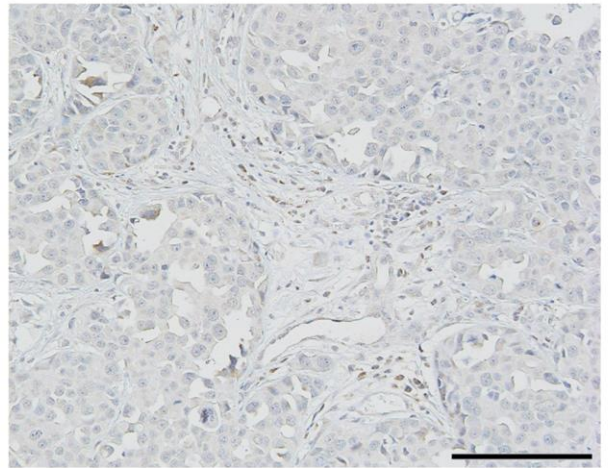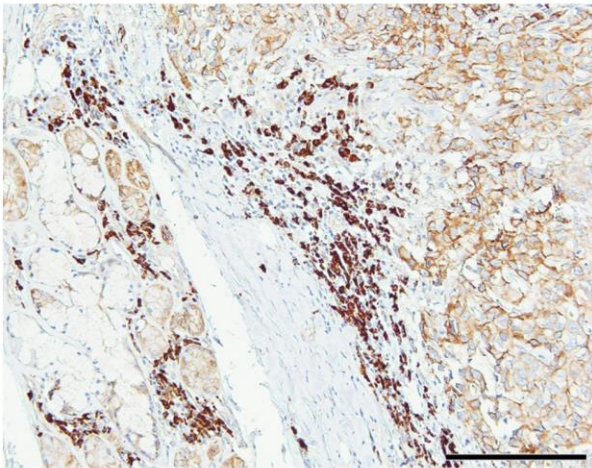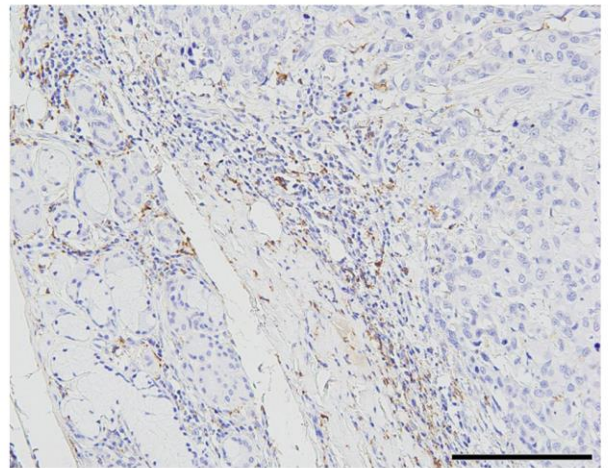
Supplementary Figure 3
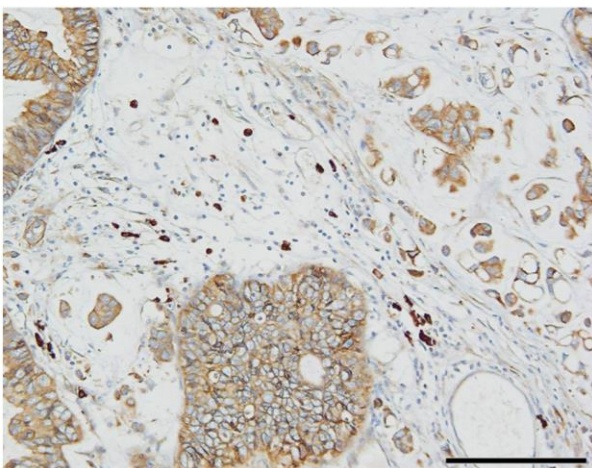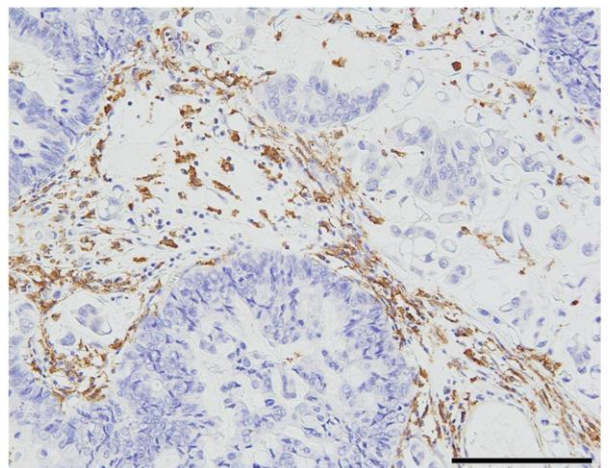

CD3 lung

NCR1 lung
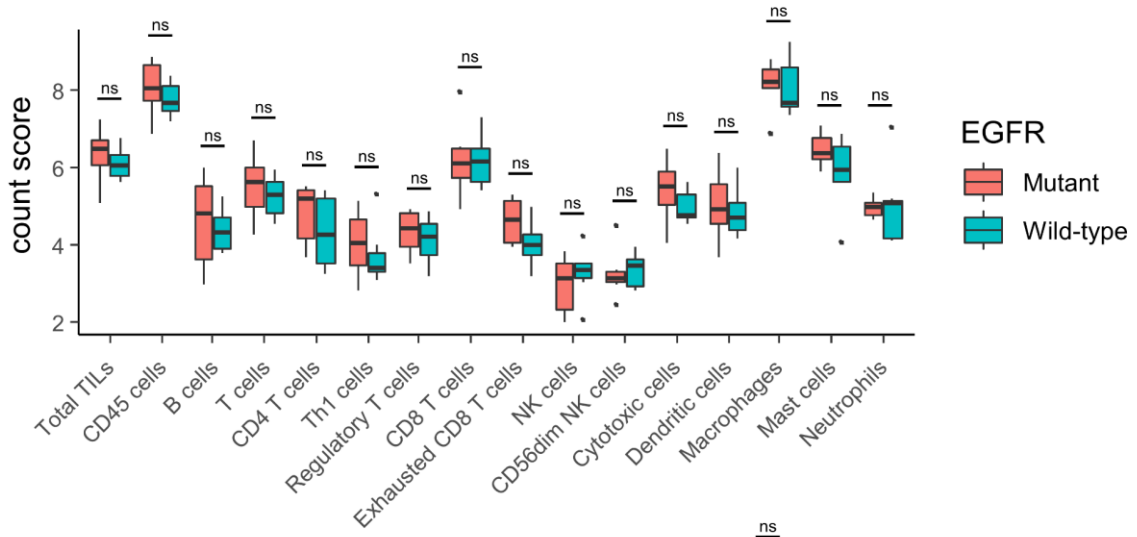
CD3 brain

NCR1 brain

iNOS lung

CD163 lung

iNOS brain

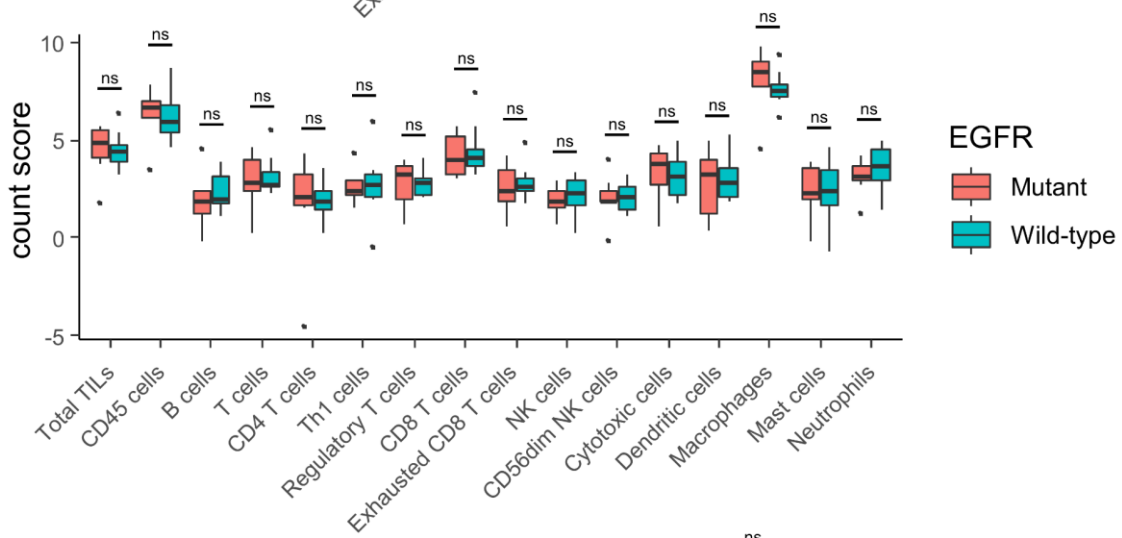CD163 brain

Supplementary Figure 4

Immune cell infiltration according to *EGFR* mutation status. a-b, Immune cell profiles of lung (**a**) and brain (**b**) samples analyzed by the NanoString method (Mann–Whitney U-test). **c-d,** Relative abundance of immune cells per total tumor-infiltrating leukocytes in lung (**c**) and brain (**d**) samples by the NanoString method (Mann–Whitney U-test). ns, not significant.
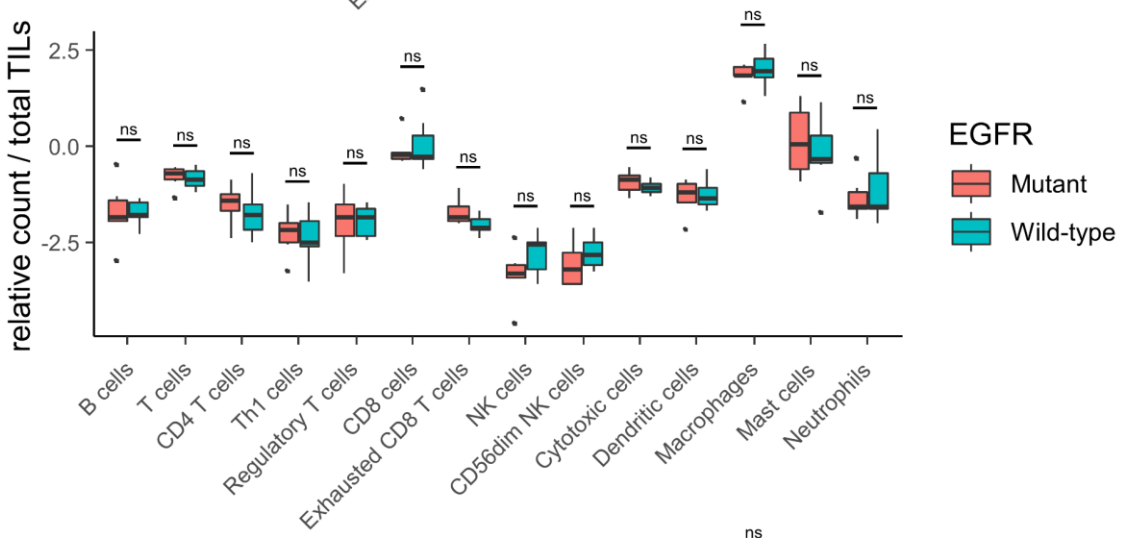
Supplementary Figure 4